Production of Peroxy Radicals from the Photochemical Reaction of Fatty Acids at the Air-Water Interface

N. Hayeck, I. Mussa, S. Perrier, C. George

Production of peroxy radicals from the photochemical reaction of fatty acids at the air-water interface

*Nathalie Hayeck[‡], Ibrahim Mussa, Sébastien Perrier, and Christian George**

Univ Lyon, Université Claude Bernard Lyon 1, CNRS, IRCELYON, F-69626, Villeurbanne, France.

ABSTRACT: Peroxy radicals are known for their role in tropospheric photochemistry as intermediates in the oxidation of volatile organic compounds, leading to the formation of ozone and organic nitrate compounds. Similarly, in the particle phase, peroxy radicals, considered a type of reactive organic species (ROS), are also involved in many chemical transformations and produce a consequential fraction of aerosols with an impact on health. Here, we show that peroxy radicals are efficiently produced at the air/water interface upon irradiation of an organic film made of a simple fatty acid (i.e., nonanoic acid). This source of peroxy radicals was quantified as 0.27 ppbv after interfacial titration of the peroxy radicals by nitric oxide in a photochemical flow reactor. Using a combination of proton transfer reaction – time of flight – mass spectrometry (PTR-ToF-MS) and ultrahigh performance liquid chromatography – heated electrospray ionization – high resolution orbitrap – mass spectrometry (UHPLC-HESI-HR Orbitrap-MS), the products of

this photochemistry were identified in the presence and absence of NO. The amount of peroxy radicals produced by this photochemistry was comparable to those measured in surface water, or the ROS bounded to ambient secondary organic aerosols. Accordingly, the photochemistry of surfactant at the air/water interface might play a significant role in the health impact of organic aerosols.

KEYWORDS Peroxy radicals, Reactive oxygen species, nonanoic acid, photochemistry, air-water interface.

1. INTRODUCTION

The oxidative capacity of the atmosphere is obviously gaining a lot of attention for its important role in controlling air quality, but also through the production of ROS due to their effects on human health[1]. The broadened definition of ROS includes oxygen-derived free radicals such as peroxy radicals ($RO_2^{\bullet}$) [1-4], which play a central role in the oxidation of volatile organic compounds (VOCs). They can react with other radicals present in the atmosphere such as NO, NO_2, HO_2 or other peroxy radicals [5], and are therefore essential in the budget of tropospheric ozone via the production of NO_2 [6]. Although this production has been known for decades, recent measurements of OH and HO_2 radicals have shown disagreements with modeled O_3 concentrations [7-9]. These findings, together with subsequent investigations, pointed toward unknown reactions involving or producing peroxy radicals as the reason for the difference between observed and modeled O_3 levels [8-11]. Recent theoretical and experimental studies have now shown that peroxy radicals also play an important role in the initiation of new particle formation via the production of highly oxygenated organic molecules (HOMs) [12-14].

Surface active compounds (i.e., surfactants) are omnipresent at air/water interfaces. In the atmosphere, those surfaces are found on aerosol particles, lakes and oceans, which cover more than 70% of the Earth [15]. Very recently, it has been shown that the surface propensity of these surfactants in the sea surface microlayer (SML), which corresponds to the uppermost layer of oceans, combined with the presence of photosensitizing compounds such as dissolved organic matter, induce unique photochemical reactions with a significant effect on the climate. This impact is materialized through their contribution to the formation of organic aerosols [16-18], the abiotic production of VOCs [19-24] or by acting as sinks for atmospheric gases such as O_3 and NO_2 [25-28]. It was also shown that even a simple monolayer of fatty acid (namely, nonanoic acid) at the air/water

interface can be photolyzed under actinic conditions, due to a slight red shift of its absorption spectrum. Such an organic film, when exposed to light in the absence of any photosensitizer, produces unsaturated and functionalized VOCs [23]. The authors suggested that these VOCs arise from complex chemistry involving the production of peroxy radicals at the air/water interface.

Here, we investigated this interfacial peroxy radical production by studying the chemistry of nitric oxide, acting as a trap for radicals at the surface of the water. This chemistry is discussed in association with the titration of $RO_2^{\bullet}$ radicals produced by the photochemistry of nonanoic acid. Moreover, the VOCs produced were identified using a proton transfer reaction time-of-flight mass spectrometer (PTR-ToF-MS). At the same time, the liquid phase composition was monitored using ultra-high performance liquid chromatography coupled to a high-resolution mass spectrometer (UHPLC-HR Orbitrap-MS).

2. EXPERIMENTAL SECTION

2.1.Photochemical reactor

The system used here is similar to the one deployed in our previous investigations [20,23]. In short, a cylindrical quartz reactor with a path length of 7 cm and an internal diameter of 1.6 cm was used as a photochemical reactor (internal volume ~14 mL). It was typically half filled with pure water with a mono to multilayer coverage of nonanoic acid. This reactor was then irradiated with a xenon arc lamp (150 W, LOT-Quantum Design, France) placed at a distance of 13 cm from the photochemical reactor to mimic the solar irradiation at the Earth's surface. To avoid excessive heating of the reactor, a quartz water filter was placed in front of the lamp to remove infrared irradiation. An additional Pyrex filter was used to eliminate the light in the UV region i.e., wavelengths lower than 290 nm. A total flow of 300 $ml \cdot min^{-1}$ of a mixture of air and NO was

continuously flowing through the reactor and analyzed using a NO_x analyzer. Identification of VOCs emitted in the gas phase was performed using commercial PTR-ToF-MS. Condensed phase products were analyzed by means of UHPLC (±) HESI-Orbitrap-MS (Figure S1).

2.2.Gas-phase measurements

NO and NO_2 concentrations were monitored simultaneously using a chemiluminescence NO detector (CLD 88p, Eco Physics, Switzerland) coupled to a photolytic converter (PLC 860, Eco Physics, Switzerland), equipped with a metal halide discharge lamp converting NO_2 to NO prior to the detection by the CLD. The NO_2 mixing ratios were corrected by the conversion factor of the photolytic converter. With this instrument, a detection limit of 0.25 ppbv was achieved.

The photochemically produced VOCs, in presence or absence of NO, were monitored using a selected reagent ion-proton transfer reaction time of flight mass spectrometer (SRI-PTR-ToF-MS 8000, Ionicon Analytik GmbH, Innsbruck, Austria) in H_3O^+ and NO^+ modes. Air was sampled at a constant flow of 100 mL/min at an inlet temperature of 60°C for both ionization modes. For the H_3O^+ mode, a drift voltage of 500 V, a drift temperature of 60°C and a drift pressure of 2 mbar were used, resulting in an E/N of about 125 Td. When NO^+ mode was used, the settings led to a low E/N of about 93 Td, which was suitable to detect nitrate organic compounds but not too low to avoid water cluster formation [29].

2.3. Condensed-phase measurements

The organic composition of the liquid phase was analyzed by ultra-high-performance liquid chromatography (Dionex 3000, Thermo Scientific, USA) coupled to a high resolution Orbitrap mass spectrometer (QExactive, Thermo Scientific, Germany). Analytes were separated on a Waters Acquity HSS T3 column (1.8 µm, 2.1 x 100 mm) using acidified water (eluent A: 0.1%, v/v, formic acid; Optima LC/MS, Fisher Scientific, USA) and acidified acetonitrile (eluent B:

0.1%, v/v, formic acid; Optima LC/MS, Fisher Scientific, USA) as the mobile phase. The QExactive was equipped with a heated electrospray ionization source (HESI) used to apply a voltage of -3.0 kV in negative mode and 3.2 kV in positive mode. The auxiliary gas flow rate was set to 25 arbitrary units (a.u.) and the sheath gas flow rate to 42 a.u. A heater temperature of 250°C and a capillary temperature of 350°C were used. The highest mass resolution of 140 000 at m/z 200 was used. A daily mass calibration was performed for the mass range of m/z 50-750 using a 2 mM of sodium acetate solution [23].

Each sample was divided into two aliquots; the first one was analyzed directly after filtration. The second one underwent a derivatization process using an excess of a PFBHA (o-(2, 3, 4, 5, 6-pentafluorobenzyl) hydroxylamine hydrochloride, Sigma Aldrich, ≥ 99.0%) in order to identify the organic compounds containing carbonyl functional groups present in the sample [30]. For this, 200 µL of the sample was mixed with 800µL of the PFBHA solution (1 mg/mL). The mixture was left in darkness at room temperature for 24 h before analysis. Three replicates of direct and derivatized analyses were assessed for each sample. Data processing and evaluation were performed using XCalibur 2.2 (Thermo, USA). Formula assignment of the identified compounds were achieved using a mass tolerance of 2 ppm.

3. RESULTS AND DISCUSSION

The production of peroxy radicals, as intermediates in the photochemistry of nonanoic acid, was assessed by the reactive uptake of nitric oxide. Effectively, when the organic fatty acid film was exposed to ~120 ppbv of NO in pure air, a decrease in the level of 1.1 ppbv NO was observed solely when the system was irradiated (Figure 1). This decrease in the NO concentration is understood as being induced by the conversion of NO by the peroxy radicals produced via the

120 photochemical reaction of nonanoic acid, as described by Rossignol et al. [23], with 1:1
121 stoichiometry. However, this NO conversion was accompanied by only a minimal increase in NO_2,
122 mostly within the noise of our detector.

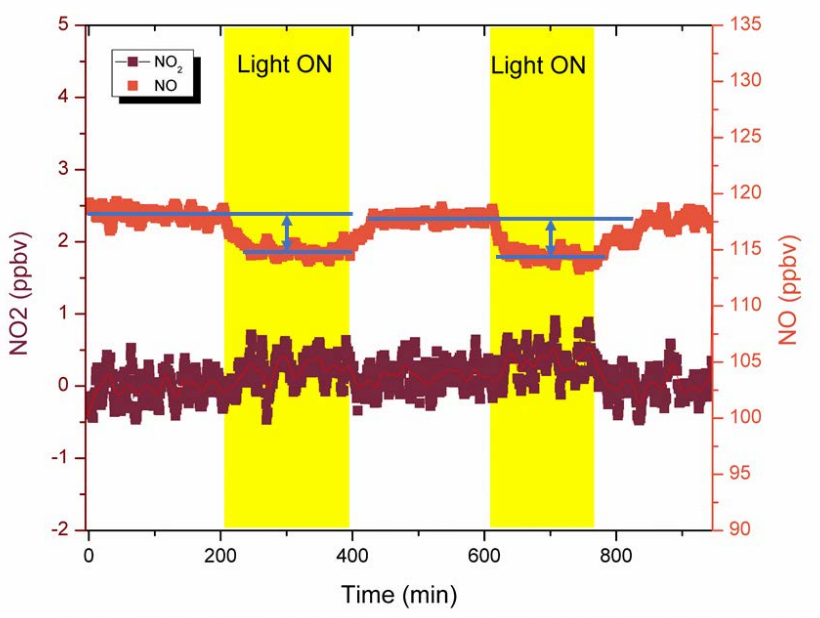

123

124 **Figure 1.** NO concentration measured in the photochemical reactor when the reactor was
125 irradiated and under dark conditions.

126 Our experimental approach did not allow us to resolve the uptake kinetics of NO, but allowed the
127 determination at steady-state (which was established very rapidly, as shown in Figure 1) of the
128 amount of NO lost at the air/water interface due to the photochemical production of peroxy
129 radicals. The amount of NO lost depends on the initial gaseous NO concentration, as shown in
130 Figure 2. Therefore, to use this information quantitatively, we performed some experiments at
131 higher concentrations, i.e. 120 ppbv NO, where the reaction between RO_2 radicals and NO
132 dominates over the self-reaction and cross-reaction of peroxy radicals, as shown by the plateau in
133 Figure 2 above 100 ppb [31,32]. At low NO mixing ratios. i.e. between 30 and 80 ppbv, the loss
134 increased (almost linearly) and levelled off at a NO mixing ratio greater than 100 ppbv. In other

words, at concentrations lower than 100 ppbv, self- and cross-reactions of RO_2 are possible, while at higher values, the NO – RO_2 reaction dominates. Therefore, a mixing ratio of 120 ppbv was used in this study to quantitatively determine the amount of peroxy radicals produced by the photochemistry of nonanoic acid.

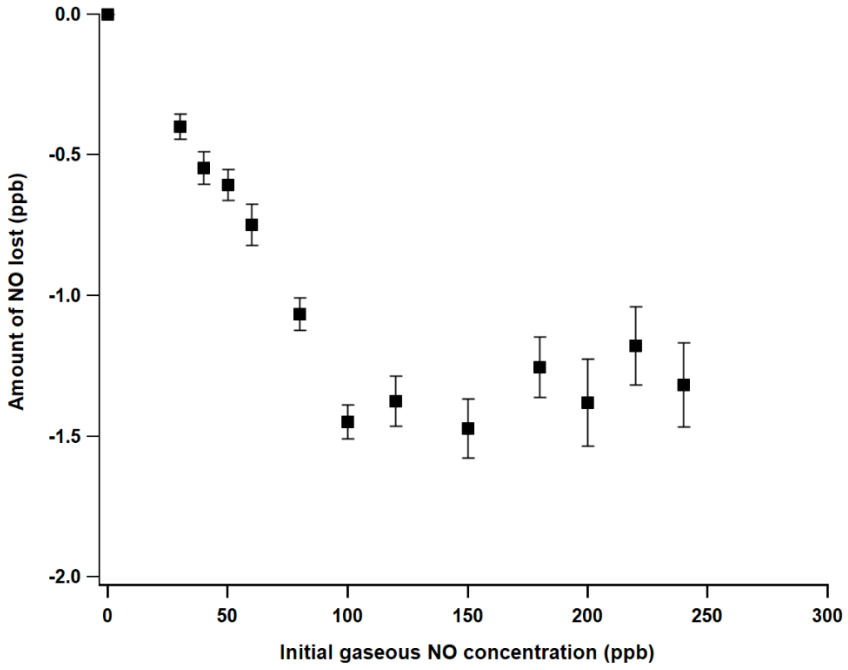

Figure 2. The amount of NO lost during the photochemical reaction as a function of the initial gaseous concentration of NO in the gas phase of the reactor.

In Figure 3, only two pathways from the mechanism suggested by Rossignol et al.[23] are represented, due to their effect on peroxy radical formation and therefore on NO uptake on irradiated nonanoic acid films. The first pathway produces a C_9-aldehyde ($C_9H_{16}O$) and OH radicals as intermediates. Since it is well-known that NO can react with $OH^{\bullet}$, any loss of NO due to this reaction should be taken into account. We therefore studied the production of this C_9-aldehyde, which is initiated by either homolytic cleavage or an inter-molecular Norrish II reaction [23]. Homolytic cleavage (reaction A) produces OH radicals, which could abstract an H atom from

a saturated aldehyde ($C_9H_{18}O$) to produce an unsaturated aldehyde ($C_9H_{16}O$). In order to investigate the possible reaction between NO and $OH^{\bullet}$, the products of the reaction involving $OH^{\bullet}$ radicals as a reagent were compared in the presence and absence of NO. An unsaturated C_9 aldehyde ($C_9H_{16}O$) was found to be present at similar amounts in both cases, as shown in Figure 4. As shown by reaction A in Figure 3, H abstraction from the saturated aldehyde can be done by an excited nonanoic acid molecule [NA]* as well. [NA]* does not compete with OH radicals since, according to a quantum chemical investigation into the photochemical reaction of nonanoic acid at an air-water interface, dehydrogenation of the saturated aldehyde by an OH radical is easier than that by an excited nonanoic acid molecule [NA]* [33]. Therefore, the formation of the unsaturated aldehyde ($C_9H_{16}O$) is due to the reaction of OH radicals with the saturated aldehyde ($C_9H_{18}O$). As shown in Figure 4, an unsaturated aldehyde is formed in the presence and absence of NO, which means that, when NO is present, OH radicals do not react with NO but rather with the saturated aldehyde ($C_9H_{18}O$) to produce the unsaturated aldehyde ($C_9H_{16}O$). Thus, the reaction between NO and OH radicals does not compete with the one between NO and carboxyperoxy radicals ($C_9H_{17}O_4^{\bullet}$).

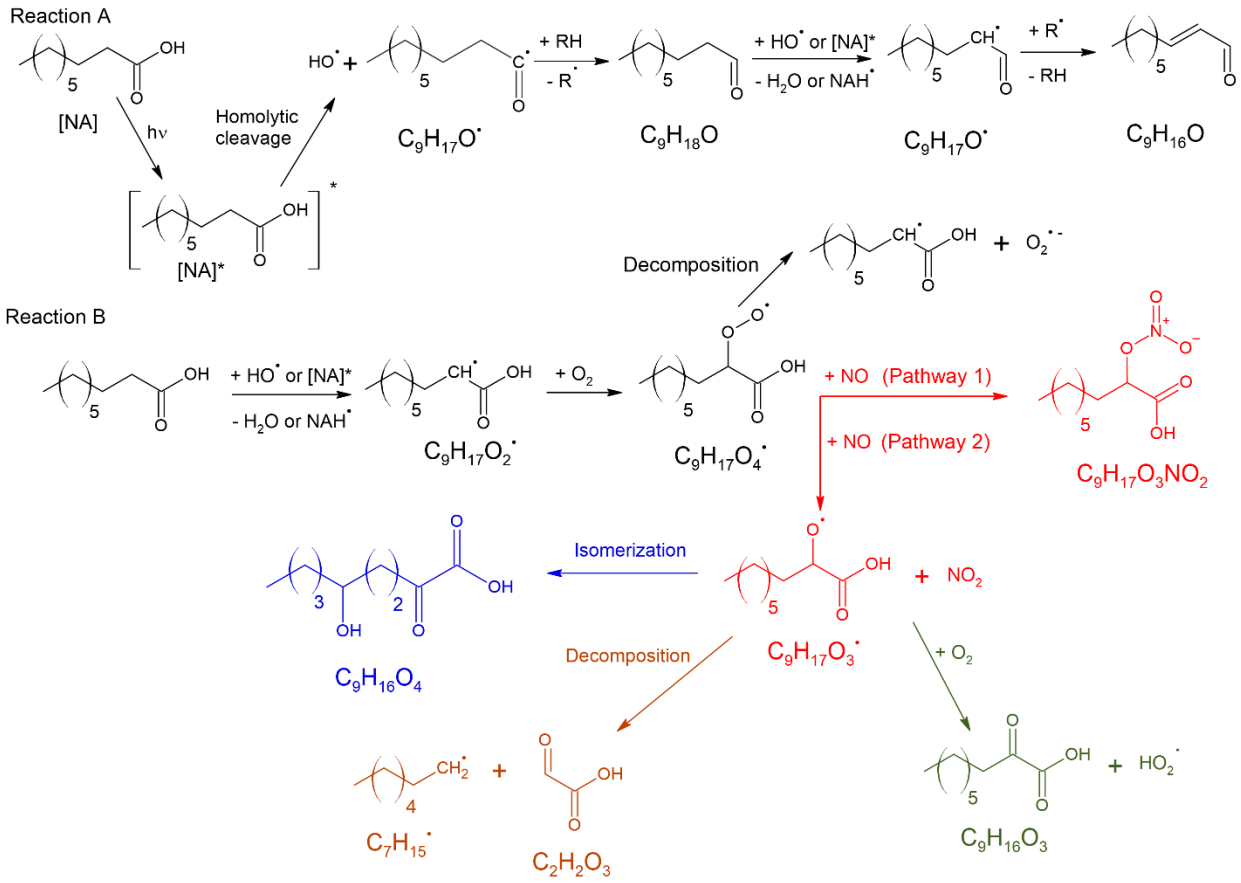

164

165 **Figure 3.** Photochemical mechanism of nonanoic acid (modified from [23]) with the possible
166 reactions of the peroxy radical with NO. [NA] represents a nonanoic acid molecule, while [NA]*
167 stands for a nonanoic acid molecule in the excited state. NAH• is a nonanoic acid molecule after
168 the abstraction of one hydrogen atom from another molecule.

169 As shown by reaction B in Figure 3, the radical $C_9H_{17}O_2^{\bullet}$ reacts with oxygen to produce the
170 carboxy peroxy radical ($C_9H_{17}O_4^{\bullet}$). As previously explained, the carboxy peroxy radical reacts
171 with NO via two pathways, which leads to the decrease in the NO concentration. In the absence of
172 oxygen, no peroxy radicals can be produced and the concentration of NO remains constant during
173 the photochemical reaction. In order to validate the presence of peroxy radicals in this
174 photochemical reaction, the same photochemical experiment was conducted in the absence of

oxygen, i.e., under pure nitrogen. The water was bubbled with a gentle nitrogen stream to remove any dissolved oxygen, and therefore prevent the formation of peroxy radicals. Figure 5 shows the changes in the amount of NO taken up when the reactor was irradiated (yellow highlight) under nitrogen or air as the dilution gas. As highlighted by the smoothed red line, a very small decrease of NO was observed when the reactor was irradiated under nitrogen. However, when air was present in the reactor, more notable uptake of NO was clearly observed. The latter confirms the role of oxygen, and possibly the formation of peroxy radicals, in NO uptake. The slight decrease in the NO mixing ratio under nitrogen could be due to the presence of a small amount of oxygen in the reactor or to the reaction of NO with $OH^{\bullet}$ produced by the first reaction with nonanoic acid.

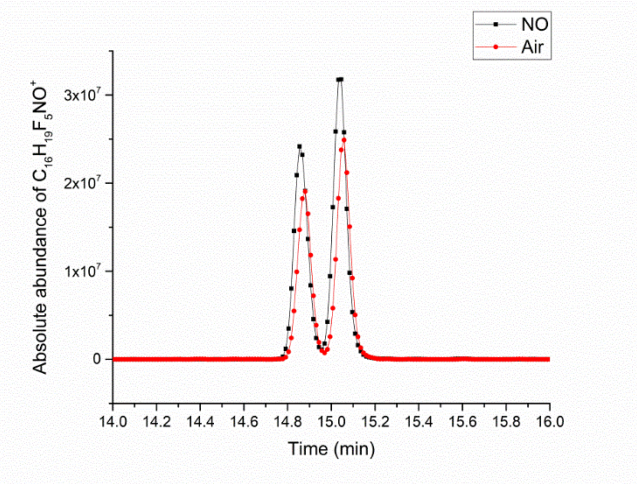

Figure 4. Chromatographic peaks corresponding to the derivatized ion of the aldehyde $C_9H_{16}O$

According to reaction B of the mechanism shown in Figure 3, the carboxy peroxy radical ($C_9H_{17}O_4^{\bullet}$) may react with NO via two pathways, or decompose [34]. The first one (pathway 1) produces complex organic nitrate compounds ($C_9H_{17}O_3NO_2$), while the second one leads to an alkoxy radical ($C_9H_{17}O_3^{\bullet}$) and NO_2, which did not increase significantly here (Figure 1).

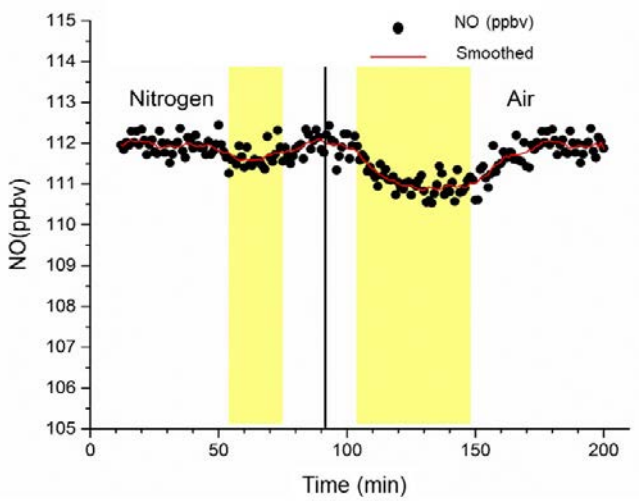

Figure 5. NO uptake under nitrogen flow on the left and air flow on the right.

However, we did not detect any organic nitrate compounds in the gas or in the liquid phases. Previous studies on gaseous alkyl nitrate formation from the reactions of C_8 – C_{14} n-alkanes with OH radicals in the presence of NO showed that the branching ratios for the formation of secondary alkyl nitrates are similar for all isomers of a particular carbon number; average values of alkyl nitrate yields were 0.219 and 0.254 for reactions of n-octane and n-dodecane, respectively. The alkyl nitrate yields increased to a plateau of 0.3 for alkyls of C_{13} and C_{14} [35]. Even though no studies have been conducted to determine the direct effect of the presence of a carboxylic group adjacent to a peroxy group, the absence of alkyl nitrate compounds in our experiments could be explained by the presence of the carboxylic group, which has a double role in reducing the alkyl nitrate yield. First, the presence of the carboxylic group may induce a net decrease in the yield of organic nitrate by a factor of 3 [36]. In addition, the presence of a hydroxyl group on an adjacent carbon (β-hydroxyperoxy) reduces the branching ratio by 46% compared to the branching ratio of an alkyl peroxy radical. These authors related this to hydrogen bonding between the hydroxy and the peroxy radical [37]. Based on these two conclusions, organonitrate production from the carboxy peroxy radical ($C_9H_{17}O_4^{\bullet}$) could be inhibited or at least reduced to very low concentrations. Since

the photochemical process studied in this work takes place at an air-water interface, the products of this reaction are expected to be divided between the gas phase and the aqueous phase. Therefore, the amounts of organonitrate present in the gas phase and the liquid phase were probably lower than the limits of detection of the PTR-ToF-MS and the HESI-Orbitrap MS, which explains the absence of any organonitrate compounds produced from the reaction of the carboxyperoxy radical and NO.

The second pathway (pathway 2 in Figure 3) in the reaction of NO with the carboxyperoxy radical was observed to be the major one, since the isomerization product ($C_9H_{16}O_4$) and the oxidation product ($C_9H_{16}O_3$) of the alkoxy radical ($C_9H_{17}O_3^{\bullet}$) were formed exclusively under NO (Figure S3 and Figure S4). These isomerization and oxidation reactions are well-documented for alkoxy radicals derived from linear and cyclic alkanes [38]. To the best of our knowledge, no studies have been conducted on carboxyalkoxy radicals. Nevertheless, our study showed the presence of the isomerization product $C_9H_{16}O_4$ having, in addition to the carboxylic function, the same functions as hydroxycarbonyls formed from the alkoxy radical isomerization reactions. This compound is produced due to the formation of a six-membered ring (cf. SI) [31,39]. The decomposition product $C_2H_2O_3$ was not detected in the samples as a product of the reaction in the presence of NO.

The detection of these products also demonstrates that the decomposition of peroxy radicals, which produces O_2^- [34], proceeds on time scales longer that the RO_2 + NO reaction. In fact, such unimolecular decomposition is enabled only for alcohols. In the case of carboxylic acids, the peroxyl group is only next to a CO_2H group and it appears that the peroxyradical is the more electronegative substituent, leading to quite slow unimolecular decomposition.

3.1. Environmental implications

In order to compare our results with field results, it is important to correct the observed loss of NO by the ratio between the real solar irradiation and the xenon lamp output in the range between 280 and 330 nm, where nonanoic acid absorbs light and reacts photochemically. Scaling down to real actinic conditions (cf. SI), and using the actual flow conditions in our reactor, and finally assuming that one NO titrates one peroxy radical, the aqueous steady-state formation rate R_f of RO_2 can be approximated by the following equation:

$$R_f \approx \frac{\Delta NO \times F_g}{V_{aq}} \quad \text{Eq. 1}$$

Where, ΔNO is the amount of NO lost (0.27 ppb), Fg the gas flow rate (300 mL min^{-1}) and finally V_{aq} the liquid volume in which the reaction takes place. This volume can be defined by two limiting cases, either the reaction takes place homogeneously in the aqueous volume of the reactor (7 mL) or in an outer shell defined by the local surface enrichment and diffusion limitations which thickness can estimate to be 100 µm similarly to the oceanic SML. Applying this equation to our conditions leads to peroxy formation rates in the range from 8×10^{-12} to 5×10^{-10} M s^{-1}. Interestingly, those data compare favorably by those reported by Faust and Hoigné [40,41] who reported midday peroxy radical formation rates in the rate from 10^{-11} to 10^{-10} M s^{-1}.

To derive the steady-state concentration of these peroxy radicals, one can estimate that in the environment their main loss corresponds to their second-order self-recombination reaction, which proceeds with a rate constant of ca. 2×10^{7} $M^{-1}s^{-1}$ [42]. In this case, the steady-state concentration can be calculated from:

$$[ROO]_{ss} = \sqrt{\frac{R_f}{2\times10^7}} \quad \text{Eq. 2}$$

leading to concentrations in the range 6×10^{-10}-6×10^{-9} M. One could then speculate that if those are in Henry's law equilibrium, then the concentration of peroxy radicals in the air aloft would be

in the range 0.006 – 0.06 ppb (assuming arbitrarily Henry's law constant of 100 M atm^{-1}, corresponding to the upper limit of reported values[43]). Several studies have been conducted to measure $RO_2^{\bullet}$ radicals in the marine boundary layer [10,44-47]. In these studies, $RO_2^{\bullet}$ radicals ranged between 0.01 and 0.05 ppbv, depending on the season, the measurement location and the air masses. Even though the values of this study are higher than those of previous work, the photochemistry of surfactants could be an important source of peroxy radicals, which may influence atmospheric chemistry models. As an example, Burkert et al. found that the atmospheric model used to simulate the total amount of $RO_2^{\bullet}$ shows a discrepancy with actual measurements. Therefore, they suggested that the presence of reactive non-methane hydrocarbons, which are not measured and included in the model, are responsible for this disagreement [24].

The experiments described above were performed on bulk solutions, and cannot therefore be applied to aerosols. Nevertheless, in an attempt to scale up the bulk concentrations given above for peroxy radicals to dispersed ultrafine particles, by normalizing the surface-to-volume ratio of our reactor to those of 200 nm diameter sized particle with an average loading of 15 µg m^{-3}, [48] we obtain a ROS loading in the range of 0.14-1.4 ppb (hereby assuming that all peroxy radicals are ROS in the condensed phase). This rough estimate is comparable to ambient particle-bound ROS (PB-ROS) measured in different cities. The ambient ROS levels measured at a polluted urban site in the UK varied between 0.098 and 0.59 ppbv of equivalent [H_2O_2] [48]. An average ROS concentration of 0.2 ppbv of equivalent [H_2O_2] was found during a study in Rochester, New York, USA in 2011 [49], which is comparable in magnitude to the concentration of ROS found in our study. Online measurements of PB-ROS in Beijing and Bern showed concentrations between 0.25 to 0.74 ppbv, and between 0.025 and 0.049 ppbv, respectively [50]. In addition, the authors found that PB-ROS are correlated with the oxygenated organic fraction. They showed that this organic aerosol

fraction contributed to more than 60% of the total PB-ROS. Considering the fact that surfactants are concentrated in the organic matrix of aerosol particles [15], this accordance in the results shows the importance of the photochemistry of fatty acids studied here in terms of ROS production and its effects on the atmosphere and human health.

4. CONCLUSION

In this work, the formation of peroxy radicals from the photochemistry of a nonanoic acid film at an air/water interface was indirectly demonstrated. The study of the gas phase and liquid phase products showed the absence of organic nitrate compounds because of the presence of the carboxyl function in the nonanoic acid. On another hand, the reaction of peroxy radicals with NO led to the formation of alkoxy radicals and subsequently new functionalized compounds formed by the oxidation and isomerization of the alkoxy radical.

The total amount of peroxy radicals produced was assessed through a titration with nitric oxide (NO). It was shown that the amount of peroxy radicals produced at the air/water interface coated with a film of nonanoic acid is comparable to the concentration of peroxy radicals found in surface water and is consistent with the fact that the SML is concentrated with organic compounds, i.e. surfactants.

This study shows the importance of surfactant photochemistry in the oxidative capacity of the atmosphere. Including the production of peroxy radicals from this photochemistry in atmospheric models might explain the difference between the modeled and measured peroxy radicals in the marine boundary layer.

ASSOCIATED CONTENT

Supporting Information. Determination of the peroxy radicals produced by the photochemical reaction of the nonanoic acid monolayer, Figure S1-S4 and Scheme S1. This material is available free of charge via the Internet at http://pubs.acs.org.

AUTHOR INFORMATION

Corresponding Author

* Dr. Christian George, CNRS-IRCELYON, 2 avenue Albert Einstein, 69626 Villeurbanne Cedex, France. Email: Christian.george@ircelyon.univ-lyon1.fr; Phone: +33 (0) 4 72 44 81 90.

Present Address

‡ Now at the Chemistry Department, Faculty of Arts and Sciences, American University of Beirut, Beirut, Lebanon.

Author Contributions

The manuscript was written with contributions from all authors. All authors have given approval to the final version of the manuscript.

Funding Sources

This study was supported by the European Research Council under the European Union's Framework Program (FP/2007-2013)/ERC Grant Agreement 290852 – AIRSEA. This project also received funding from the European Union's Horizon 2020 research and innovation program under grant agreement No. 690958 (MARSU).

Notes

The authors declare no competing financial interests.

Acknowledgments

The authors are thankful to Nicolas Charbonnel for the technical support provided.

Abbreviations

ROS, Reactive Oxygen Species; VOCs, Volatile Organic Compounds; HOM, Highly Oxygenated Organic Molecules; SML, Sea Surface Microlayer; PTR-ToF-MS, Proton Transfer Reaction Time-of-Flight Mass Spectrometry; UHPLC-HR Orbitrap-MS, Ultra-high Performance Liquid Chromatography High Resolution Mass Spectrometry; HESI, Heated Electrospray Ionization Source; PFBHA, o-(2, 3, 4, 5, 6-pentafluorobenzyl) hydroxylamine; PB-ROS, Particle Bound Reactive Oxygen Species

REFERENCES

1, Pöschl, U.; Shiraiwa, M. Multiphase Chemistry at the Atmosphere–Biosphere Interface Influencing Climate and Public Health in the Anthropocene. Chem. Rev. **2015**, *115* (10), 4440–4475. https://doi.org/10.1021/cr500487s.

2. Anglada, J. M.; Martins-Costa, M.; Francisco, J. S.; Ruiz-López, M. F. Interconnection of Reactive Oxygen Species Chemistry across the Interfaces of Atmospheric, Environmental, and Biological Processes. Acc. Chem. Res. **2015**, *48* (3), 575–583. https://doi.org/10.1021/ar500412p.

3. Birben, E.; Sahiner, U. M.; Sackesen, C.; Erzurum, S.; Kalayci, O. Oxidative Stress and Antioxidant Defense: World Allergy Organ. J. **2012**, *5* (1), 9–19. https://doi.org/10.1097/WOX.0b013e3182439613.

4. Winterbourn, C. C. Reconciling the Chemistry and Biology of Reactive Oxygen Species. Nat. Chem. Biol. **2008**, *4* (5), 278–286. https://doi.org/10.1038/nchembio.85.

5. Mellouki, A.; Wallington, T. J.; Chen, J. Atmospheric Chemistry of Oxygenated Volatile Organic Compounds: Impacts on Air Quality and Climate. Chem. Rev. **2015**, *115* (10), 3984–4014. https://doi.org/10.1021/cr500549n.

6. Pusede, S. E.; Steiner, A. L.; Cohen, R. C. Temperature and Recent Trends in the Chemistry of Continental Surface Ozone. Chem. Rev. **2015**, *115* (10), 3898–3918. https://doi.org/10.1021/cr5006815.

7. Martinez, M.; Harder, H.; Kubistin, D.; Rudolf, M.; Bozem, H.; Eerdekens, G.; Fischer, H.; Konigstedt, R.; Parchatka, U.; Schiller, C. L.; Stickler, A.; Williams, J.; Lelieveld, J. Hydroxyl Radicals in the Tropical Troposphere over the Suriname Rainforest: Airborne Measurements. Atmos Chem Phys **2010**, *15*, 3759-3773.

8. Hofzumahaus, A.; Rohrer, F.; Lu, K.; Bohn, B.; Brauers, T.; Chang, C.-C.; Fuchs, H.; Holland, F.; Kita, K.; Kondo, Y.; Li, X.; Lou, S.; Shao, M.; Zeng, L.; Wahner, A.; Zhang, Y. Amplified Trace Gas Removal in the Troposphere. Science **2009**, *324* (5935), 1702–1704. https://doi.org/10.1126/science.1164566.

9. Lelieveld, J.; Butler, T. M.; Crowley, J. N.; Dillon, T. J.; Fischer, H.; Ganzeveld, L.; Harder, H.; Lawrence, M. G.; Martinez, M.; Taraborrelli, D.; Williams, J. Atmospheric Oxidation Capacity Sustained by a Tropical Forest. Nature **2008**, *452* (7188), 737–740. https://doi.org/10.1038/nature06870.

10. Burkert, J.; Andrés-Hernández, M. D.; Reichert, L.; Meyer-Arnek, J.; Doddridge, B.; Dickerson, R. R.; Mühle, J.; Zahn, A.; Carsey, T.; Burrows, J. P. Trace Gas and Radical Diurnal Behavior in the Marine Boundary Layer during INDOEX 1999. J. Geophys. Res. Atmospheres **2003**, *108* (D8). https://doi.org/10.1029/2002JD002790.

11. Nozière, B.; Kalberer, M.; Claeys, M.; Allan, J.; D'Anna, B.; Decesari, S.; Finessi, E.; Glasius, M.; Grgić, I.; Hamilton, J. F.; Hoffmann, T.; Iinuma, Y.; Jaoui, M.; Kahnt, A.; Kampf, C. J.; Kourtchev, I.; Maenhaut, W.; Marsden, N.; Saarikoski, S.; Schnelle-Kreis, J.; Surratt, J. D.; Szidat, S.; Szmigielski, R.; Wisthaler, A. The Molecular Identification of Organic Compounds in the Atmosphere: State of the Art and Challenges. Chem. Rev. **2015**, *115* (10), 3919–3983. https://doi.org/10.1021/cr5003485.

12. Roldin, P.; Ehn, M.; Kurtén, T.; Olenius, T.; Rissanen, M. P.; Sarnela, N.; Elm, J.; Rantala, P.; Hao, L.; Hyttinen, N.; Heikkinen, L.; Worsnop, D. R.; Pichelstorfer, L.; Xavier, C.; Clusius, P.; Öström, E.; Petäjä, T.; Kulmala, M.; Vehkamäki, H.; Virtanen, A.; Riipinen, I.; Boy, M. The Role of Highly Oxygenated Organic Molecules in the Boreal Aerosol-Cloud-Climate System. Nat. Commun. **2019**, *10* (1), 4370. https://doi.org/10.1038/s41467-019-12338-8.

13. Schervish, M.; Donahue, N. M. Peroxy Radical Chemistry and the Volatility Basis Set; preprint; Gases/Atmospheric Modelling/Troposphere/Chemistry (chemical composition and reactions), 2019. https://doi.org/10.5194/acp-2019-509.

14. Zhao, Y.; Thornton, J. A.; Pye, H. O. T. Quantitative Constraints on Autoxidation and Dimer Formation from Direct Probing of Monoterpene-Derived Peroxy Radical Chemistry. Proc. Natl. Acad. Sci. **2018**, *115* (48), 12142–12147. https://doi.org/10.1073/pnas.1812147115.

15. George, C.; Ammann, M.; D'Anna, B.; Donaldson, D. J.; Nizkorodov, S. A. Heterogeneous Photochemistry in the Atmosphere. Chem. Rev. **2015**, *115* (10), 4218–4258. https://doi.org/10.1021/cr500648z.

16. Alpert, P. A.; Ciuraru, R.; Rossignol, S.; Passananti, M.; Tinel, L.; Perrier, S.; Dupart, Y.; Steimer, S. S.; Ammann, M.; Donaldson, D. J.; George, C. Fatty Acid Surfactant Photochemistry Results in New Particle Formation. Sci. Rep. **2017**, *7* (1). https://doi.org/10.1038/s41598-017-12601-2.

17. Bernard, F.; Ciuraru, R.; Boréave, A.; George, C. Photosensitized Formation of Secondary Organic Aerosols above the Air/Water Interface. Environ. Sci. Technol. **2016**, *50* (16), 8678–8686. https://doi.org/10.1021/acs.est.6b03520.

18. Brüggemann, M.; Hayeck, N.; George, C. Interfacial Photochemistry at the Ocean Surface Is a Global Source of Organic Vapors and Aerosols. Nat. Commun. **2018**, *9* (1). ,https://doi.org/10.1038/s41467-018-04528-7.

19. Brüggemann, M.; Hayeck, N.; Bonnineau, C.; Pesce, S.; Alpert, P. A.; Perrier, S.; Zuth, C.; Hoffmann, T.; Chen, J.; George, C. Interfacial Photochemistry of Biogenic Surfactants: A Major Source of Abiotic Volatile Organic Compounds. Faraday Discuss. **2017**, *200*, 59–74. https://doi.org/10.1039/C7FD00022G.

20. Ciuraru, R.; Fine, L.; van Pinxteren, M.; D'Anna, B.; Herrmann, H.; George, C. Photosensitized Production of Functionalized and Unsaturated Organic Compounds at the Air-Sea Interface. Sci. Rep. **2015**, *5* (1). https://doi.org/10.1038/srep12741.

21. Ciuraru, R.; Fine, L.; Pinxteren, M. van; D'Anna, B.; Herrmann, H.; George, C. Unravelling New Processes at Interfaces: Photochemical Isoprene Production at the Sea Surface. Environ. Sci. Technol. **2015**, *49* (22), 13199–13205. https://doi.org/10.1021/acs.est.5b02388.

22. Fu, H.; Ciuraru, R.; Dupart, Y.; Passananti, M.; Tinel, L.; Rossignol, S.; Perrier, S.; Donaldson, D. J.; Chen, J.; George, C. Photosensitized Production of Atmospherically Reactive Organic Compounds at the Air/Aqueous Interface. J. Am. Chem. Soc. **2015**, *137* (26), 8348–8351. https://doi.org/10.1021/jacs.5b04051.

23. Rossignol, S.; Tinel, L.; Bianco, A.; Passananti, M.; Brigante, M.; Donaldson, D. J.; George, C. Atmospheric Photochemistry at a Fatty Acid–Coated Air-Water Interface. Science **2016**, *353* (6300), 699–702. https://doi.org/10.1126/science.aaf3617.

24. Tinel, L.; Rossignol, S.; Bianco, A.; Passananti, M.; Perrier, S.; Wang, X.; Brigante, M.; Donaldson, D. J.; George, C. Mechanistic Insights on the Photosensitized Chemistry of a Fatty Acid at the Air/Water Interface. Environ. Sci. Technol. **2016**, *50* (20), 11041–11048. https://doi.org/10.1021/acs.est.6b03165.

25. Carpenter, L. J.; Nightingale, P. D. Chemistry and Release of Gases from the Surface Ocean. Chem. Rev. **2015**, *115* (10), 4015–4034. https://doi.org/10.1021/cr5007123.

26. George, C.; Ammann, M.; D'Anna, B.; Donaldson, D. J.; Nizkorodov, S. A. Heterogeneous Photochemistry in the Atmosphere. Chem. Rev. **2015**, *115* (10), 4218–4258. https://doi.org/10.1021/cr500648z.

27. Jammoul, A.; Dumas, S.; D'Anna, B.; George, C. Photoinduced Oxidation of Sea Salt Halides by Aromatic Ketones: A Source of Halogenated Radicals. Atmos Chem Phys **2009**, *9*, 4229–4237

28. Reeser, D. I.; Jammoul, A.; Clifford, D.; Brigante, M.; D'Anna, B.; George, C.; Donaldson, D. J. Photoenhanced Reaction of Ozone with Chlorophyll at the Seawater Surface. J. Phys. Chem. C **2009**, *113* (6), 2071–2077. https://doi.org/10.1021/jp805167d.

29. Duncianu, M.; David, M.; Kartigueyane, S.; Cirtog, M.; Doussin, J.-F.; Picquet-Varrault, B. Measurement of Alkyl and Multifunctional Organic Nitrates by Proton-Transfer-Reaction Mass Spectrometry. Atmospheric Meas. Tech. **2017**, *10* (4), 1445–1463. https://doi.org/10.5194/amt-10-1445-2017.

30. Borrás, E.; Tortajada-Genaro, L. A. Determination of Oxygenated Compounds in Secondary Organic Aerosol from Isoprene and Toluene Smog Chamber Experiments. Int. J. Environ. Anal. Chem. **2012**, *92* (1), 110–124. https://doi.org/10.1080/03067319.2011.572164.

31. Atkinson, R. Gas-Phase Tropospheric Chemistry of Volatile Organic Compounds: 1. Alkanes and Alkenes. J. Phys. Chem. Ref. Data **1997**, *26* (2), 215–290. https://doi.org/10.1063/1.556012.

32. Ziemann, P. J.; Atkinson, R. Kinetics, Products, and Mechanisms of Secondary Organic Aerosol Formation. Chem. Soc. Rev. **2012**, *41* (19), 6582–6605. https://doi.org/10.1039/C2CS35122F.

33. Xiao, P.; Wang, Q.; Fang, W.-H.; Cui, G. Quantum Chemical Investigation on Photochemical Reactions of Nonanoic Acids at Air–Water Interface. J. Phys. Chem. A **2017**, *121* (22), 4253–4262. https://doi.org/10.1021/acs.jpca.7b03123.

34. Sonntag, C. von; Schuchmann, H.-P. The Elucidation of Peroxyl Radical Reactions in Aqueous Solution with the Help of Radiation-Chemical Methods. Angew. Chem. Int. Ed. Engl. **1991**, *30* (10), 1229–1253. https://doi.org/10.1002/anie.199112291.

35. Yeh, G. K.; Ziemann, P. J. Alkyl Nitrate Formation from the Reactions of C8-C14 n-Alkanes with OH Radicals in the Presence of NO(x): Measured Yields with Essential Corrections for Gas-Wall Partitioning. J. Phys. Chem. A **2014**, *118* (37), 8147–8157. https://doi.org/10.1021/jp500631v.

36. Espada, C.; Grossenbacher, J.; Ford, K.; Couch, T.; Shepson, P. B. The Production of Organic Nitrates from Various Anthropogenic Volatile Organic Compounds. Int. J. Chem. Kinet. **2005**, *37* (11), 675–685. https://doi.org/10.1002/kin.20122.

37. Matsunaga, A.; Ziemann, P. J. Yields of β-Hydroxynitrates and Dihydroxynitrates in Aerosol Formed from OH Radical-Initiated Reactions of Linear Alkenes in the Presence of NO x. J. Phys. Chem. A **2009**, *113* (3), 599–606. https://doi.org/10.1021/jp807764d.

38. Kwok, E. S. C.; Arey, J.; Atkinson, R. Alkoxy Radical Isomerization in the OH Radical-Initiated Reactions of C4-C8 n-Alkanes. J. Phys. Chem. **1996**, *100* (1), 214–219. https://doi.org/10.1021/jp952036x.

39. Atkinson, R.; Kwok, E. S. C.; Arey, J.; Aschmann, S. M. Reactions of Alkoxyl Radicals in the Atmosphere. Faraday Discuss. **1995**, *100*, 23. https://doi.org/10.1039/fd9950000023.

40. Faust, B. C.; Hoigne, J. Sensitized Photooxidation of Phenols by Fulvic Acid and in Natural Waters. Environ. Sci. Technol. **1987**, *21* (10), 957–964.

41. Blough, N.V.; Zepp, R. G. Reactive Oxygen Species in Natural Waters. In *Active Oxygen in Chemistry*; Foote, C. S., Valentine, J. S., Greenberg, A., Liebman, J. F., Ed.; Structure energetics and reactivity in chemistry series; Blackie Academic & Professional: London; New York, 1995.

42. Sonntag, C.V.; Schumann, H.P. The Elucidation of Peroxyl Radical Reactions in Aqueous Solution with the Help of Radiation-Chemical Methods. Angewandte Chemie Int. **1991,** *30*, 10. https://doi.org/10.1002/anie.199112291

43. Sander, R.; Compilation of Henry's law constants (version 4.0) for water as solvent. Atmos. Chem. Phys. **2015,** *15*, 4399-4981

44. Burkert, J.; Andrés-Hernández, M.-D.; Stöbener, D.; Burrows, J. P.; Weissenmayer, M.; Kraus, A. Peroxy Radical and Related Trace Gas Measurements in the Boundary Layer above the Atlantic Ocean. J. Geophys. Res. Atmospheres **2001**, *106* (D6), 5457–5477. https://doi.org/10.1029/2000JD900613.

45. Fleming, Z. L.; Monks, P. S.; Rickard, A. R.; Bandy, B. J.; Brough, N.; Green, T. J.; Reeves, C. E.; Penkett, S. A. Seasonal Dependence of Peroxy Radical Concentrations at a Northern Hemisphere Marine Boundary Layer Site during Summer and Winter: Evidence for Radical Activity in Winter. Atmospheric Chem. Phys. **2006**, *6* (12), 5415–5433.

46. Fleming, Z. L.; Monks, P. S.; Rickard, A. R.; Heard, D. E.; Bloss, W. J.; Seakins, P. W.; Still, T. J.; Sommariva, R.; Pilling, M. J.; Morgan, R. Peroxy Radical Chemistry and the Control

of Ozone Photochemistry at Mace Head, Ireland during the Summer of 2002. Atmospheric Chem. Phys. **2006**, *6* (8), 2193–2214.

47. Monks, P. Fundamental Ozone Photochemistry in the Remote Marine Boundary Layer the Soapex Experiment, Measurement and Theory. Atmos. Environ. **1998**, *32* (21), 3647–3664. https://doi.org/10.1016/S1352-2310(98)00084-3.

48. Wragg, F. P. H.; Fuller, S. J.; Freshwater, R.; Green, D. C.; Kelly, F. J.; Kalberer, M. An Automated Online Instrument to Quantify Aerosol-Bound Reactive Oxygen Species (ROS) for Ambient Measurement and Health-Relevant Aerosol Studies. Atmospheric Meas. Tech. **2016**, *9* (10), 4891–4900. https://doi.org/10.5194/amt-9-4891-2016.

49. Wang, Y.; Hopke, P. K.; Sun, L.; Chalupa, D. C.; Utell, M. J. Laboratory and Field Testing of an Automated Atmospheric Particle-Bound Reactive Oxygen Species Sampling-Analysis System. J. Toxicol. **2011**, *2011*, 1–9. https://doi.org/10.1155/2011/419476.

50. Zhou, J.; Elser, M.; Huang, R.-J.; Krapf, M.; Fröhlich, R.; Bhattu, D.; Stefenelli, G.; Zotter, P.; Bruns, E. A.; Pieber, S. M.; Ni, H.; Wang, Q.; Wang, Y.; Zhou, Y.; Chen, C.; Xiao, M.; Slowik, J. G.; Brown, S.; Cassagnes, L.-E.; Daellenbach, K. R.; Nussbaumer, T.; Geiser, M.; Prévôt, A. S. H.; El-Haddad, I.; Cao, J.; Baltensperger, U.; Dommen, J. Predominance of Secondary Organic Aerosol to Particle-Bound Reactive Oxygen Species Activity in Fine Ambient Aerosol. Atmospheric Chem. Phys. **2019**, *19* (23), 14703–14720. https://doi.org/10.5194/acp-19-14703-2019.

502

503

504